ISSN 0006-2979, Biochemistry (Moscow), 2011, Vol. 76, No. 5, pp. 497-516. © Pleiades Publishing, Ltd., 2011.
Original Russian Text © I. V. Perevoshchikova, E. A. Kotova, Y. N. Antonenko, 2011, published in Biokhimiya, 2011, Vol. 76, No. 5, pp. 613-635.

REVIEW

Fluorescence Correlation Spectroscopy in Biology, Chemistry, and Medicine

I. V. Perevoshchikova[1,2], E. A. Kotova[1], and Y. N. Antonenko[1]*

[1]*Belozersky Institute of Physico-Chemical Biology, Lomonosov Moscow State University, 119991 Moscow, Russia; fax: (495) 939-3181; E-mail: antonen@genebee.msu.ru*
[2]*Department of Biomedical Sciences, University of Veterinary Medicine, Vienna, Austria*

Received October 15, 2010
Revision received November 24, 2010

Abstract—This review describes the method of fluorescence correlation spectroscopy (FCS) and its applications. FCS is used for investigating processes associated with changes in the mobility of molecules and complexes and allows researchers to study aggregation of particles, binding of fluorescent molecules with supramolecular complexes, lipid vesicles, etc. The size of objects under study varies from a few angstroms for dye molecules to hundreds of nanometers for nanoparticles. The described applications of FCS comprise various fields from simple chemical systems of solution/micelle to sophisticated regulations on the level of living cells. Both the methodical bases and the theoretical principles of FCS are simple and available. The present review is concentrated preferentially on FCS applications for studies on artificial and natural membranes. At present, in contrast to the related approach of dynamic light scattering, FCS is poorly known in Russia, although it is widely employed in laboratories of other countries. The goal of this review is to promote the development of FCS in Russia so that this technique could occupy the position it deserves in modern Russian science.

DOI: 10.1134/S0006297911050014

Key words: fluorescence fluctuations, correlation spectroscopy, diffusion, aggregation, binding, nanoparticles, biopolymers, vesicles, ligands, receptors, conformational changes, nucleic acid and protein folding

The modern science is characterized by a gradual development from studies of objects on the macro level (an object as a whole) to studies of properties of nanoobjects and even of single molecules. This general thesis can be applied to modern biochemistry and biophysics, which now use such approaches to study biomolecules as atomic force microscopy, fluorescence microscopy of single molecules, measurement of single channel activities, and some others. Fluorescence correlation spectroscopy (FCS) is based on recording fluorescence fluctuations of single particles arising as a result of Brownian motion inside a small laser-illuminated volume (confocal volume). Modern objectives can focus a laser beam into a spot of fractions of a micron in size and record a signal from a volume of ~10^{-15} liter. Time dependence of the fluorescence intensity $F(t)$ of fluorescent molecules in solution or of particles of a dispersed phase is characterized by appearance of signal fluctuations (jumps) on the background of a virtually constant basal level signal with low amplitude. Each jump corresponds to passing of an individual particle across the confocal volume. Note that the amplitude of fluorescence fluctuations is determined by the number of fluorophore molecules bound with the particle and does not depend on the particle size. The standard processing of the time dependence of fluorescence fluctuations as an autocorrelation function ($G(\tau)$) gives information about two important parameters: particle diffusion time (τ_d), which is directly proportional to their size, and the number of particles within the confocal volume (N). FCS is traditionally used to study processes associated with changes in the mobility of molecules and complexes, including particle aggregation and interactions of fluorescent particles with supramolecular complexes, lipid vesicles, etc., and the size of objects under study varies very widely – from a few angstroms for dye molecules to hundreds of nanometers for nanoparticles.

FCS is actively used in laboratories throughout the world, but for some unclear reason it is poorly known in

Abbreviations: DNP, 2,4-dinitrophenol; FCS, fluorescence correlation spectroscopy; $G(\tau)$, autocorrelation function; PCH, photon counting histogram; TMRE, tetramethylrhodamine ethyl ester; τ_d, diffusion time.

* To whom correspondence should be addressed.

Russia, although in the late 1970s a world-class FCS set-up was created in the USSR, in the Institute of Chemical and Biological Physics, Academy of Sciences of the Estonian Soviet Socialist Republic (Tallinn) [1, 2], which was used to obtain fundamentally new results [3-7]. On the background of the voluminous world literature on FCS, which in addition to experimental and theoretical papers includes many reviews [8-21], there are only a small number of current publications in Russian [22-27], and one of these works was been performed entirely in a British laboratory [24]. FCS is essentially very similar to photon correlation spectroscopy (also called dynamic light scattering), which is widely used in Russia for measurement of size of nanoparticles in suspension.

The purpose of the present review is to fill a void in information in Russia about the FCS method. The authors have constructed a FCS set-up in their laboratory and have obtained their own experience in the efficiency and fruitfulness of this approach.

HISTORY OF DEVELOPMENT OF THE METHOD

FCS is an experimental method based on statistical processing of fluorescence fluctuations when a small number of dye molecules are to be recorded. In contrast to other methods recording a fluorescence signal, in FCS not the fluorescence intensity signal itself is the most informative but its deviation from the middle value, i.e. fluorescence fluctuations. The subsequent autocorrelation of the time signal can give information about the diffusion coefficient and particle concentration. Just this mathematical transformation gave the name to the method. Initially, the method was created to study kinetics of chemical reactions. In 1972 Magde et al. [28] revealed that the new method could be used to study the binding of ethidium bromide (EtBr) with a double-stranded DNA molecule:

$$\mathrm{EtBr + DNA} \underset{k_{diss}}{\overset{k_{bind}}{\longleftrightarrow}} \mathrm{EtBr{\cdot}DNA}.$$

EtBr is a small fluorescent molecule capable of intercalating between DNA bases that is accompanied by a 20-fold increase in the quantum yield of its fluorescence.

Initially, the set-up included an argon laser with wavelength of 514.5 nm. The fluorescence was collected with a parabolic mirror, passed through a solution of $K_2Cr_2O_7$ for blocking the exciting light, and was collected onto a photoelectron multiplier. Then the analog fluorescence signal was analyzed with a 100-channel correlator. Typical concentrations of the preparations were 5 μM EtBr and 5 nM 20-kDa DNA from calf thymus.

Dimensions of the observation region were 5 μm in the transversal and 150 μm in the longitudinal direction. Thus, the observation field comprised 10^4 molecules. Processing with a correlator of the signal of the fluorescence fluctuations resulted in an autocorrelation function with diffusion times of 10-100 msec. In the described system fluorescence fluctuations arose as a result of two processes: free diffusion of fluorescent molecules in the observation volume, and the interaction of fluorescent molecules with DNA leading to increase in fluorescence. Analysis of autocorrelation functions obtained for different EtBr concentrations resulted in values of binding and dissociation constants of the complexes, which were equal, respectively, to $1.5{\cdot}10^7$ $M^{-1}{\cdot}sec^{-1}$ and 27 sec^{-1} [28].

The subsequent theoretical and experimental development of the method [29-31] promoted the application of FCS to determine constants of chemical reactions, particle concentration, molecule aggregation, and rotational and translational movement in two- and three-dimensional space [5, 6, 29-36]. The method was successfully applied to study lipid diffusion in membranes [35, 37, 38]. The diffusion coefficient $D = 9.9{\cdot}10^{-8}$ cm^2/sec was determined for a fluorescent molecule of 3,3′-dioctadecylindocarbocyanine iodide (DiI) in an artificial bilayer lipid membrane formed from egg lecithin and cholesterol at the molar ratio of 2 : 1. However, the first set-ups had a poor signal/noise ratio mainly because of the low sensitivity of the detector, the presence of a large number of particles in the laser-illuminated volume, and insufficient suppression of the background signal.

The single-molecule detection technique combined with the confocal principle in the works of Rigler et al. [39] was a great step forward. It opened the possibility for studies of processes not only in aqueous solution, but also within intact cells [9, 39, 40].

In the case of one-photon laser excitation, a modern FCS set-up (Fig. 1) allows the laser beam to pass through the lens system and to enlarge in diameter to 6-8 mm. Then the exciting light is directed into the microscope objective via a dichroic mirror (a wavelength-selective mirror) and is focused in a sample. Usually a water immersion objective with numerical aperture (NA) > 0.9 is used. The sample fluorescence is collected by the same objective and is passed through a dichroic mirror, which separates it from the exciting light. To isolate the fluorescence wavelength, emission filters are additionally used. A confocal diaphragm (pinhole) on the image surface limits the passage of the fluorescence signal and provides for collecting the light only from the confocal volume. In the scheme presented the light-guide end-wall is used as a diaphragm. Then the fluorescence photons fall onto a detector, preferentially an avalanche photodiode or photomultiplier, which records single photons. Then the signal is converted by a special computer board functioning as a correlator. By choosing the confocal diaphragm diameter, dimensions of the recorded confocal region were decreased to 0.32 μm in the transversal and to 1.53 μm in the longitudinal direction [39].

In some modern FCS set-ups a two-photon excitation is used, which makes possible the excitation at the

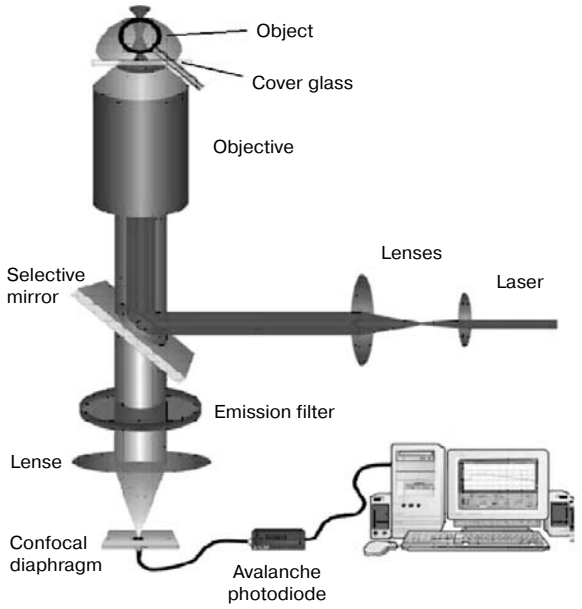

Fig. 1. Principle of operation of set-up for fluorescence correlation spectroscopy.

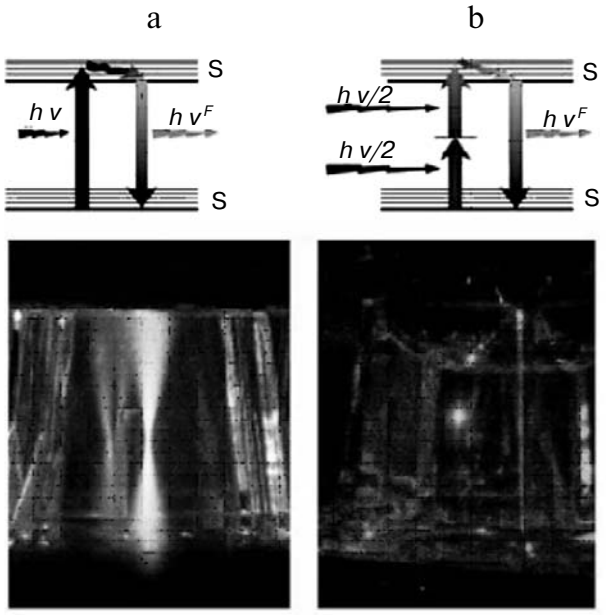

Fig. 2. Illuminated region obtained using a one-photon (a) and two-photon (b) laser excitation.

doubled wavelength as compared to the usual excitation spectrum of the dye fluorescence (Fig. 2). The probability of absorption of two photons by the same molecule is proportional to square of the radiation intensity. This leads to isolation of a very small volume near the focal surface where due to the maximal intensity of the exciting light the two-photon excitation of molecules occurs, on one hand, and they can be irreversibly bleached, on the other hand. These features of the two-photon excitation are very advantageous for measurements within cells [41, 42]. In contrast, the one-photon excitation is associated with bleaching of a significant number of fluorescent molecules upwards and downwards from the confocal volume. In the case of the two-photon laser excitation, no confocal diaphragm is required and the total flux of fluorescence photons directly falls onto the photoelectron multiplier, then onto the amplifier, and then onto the correlation board. Unfortunately, the high price of lasers used for the two-photon excitation markedly prevents their use in practice.

In 1974 Koppel [43] for the first time statistically analyzed standard deviations of experimental autocorrelation curves. Consideration of influences of different factors (detector characteristics, confocal volume size and shape, concentration of particles in the confocal volume, laser radiation intensity, etc.) on the recorded signal promoted the further development of theoretical analysis [40, 44, 45]. Different applications of FCS were developed for analysis of particles with the same or similar diffusion coefficients [46-49]. Such works enlarged the fields for using the method for studies on different biological objects.

Alongside other methods of confocal fluorescence microscopy, FCS is today a standard approach that is rather simple in practice and is characterized by a high time and spatial resolution permitting the recording of signals on the level of single molecules.

EXPERIMENTAL AND THEORETICAL BASES OF THE METHOD

Confocal volume and approaches for its determination. The confocal principle widely used in modern microscopy is an important component in current applications of the FCS method. The term "confocal" corresponds to locating a confocal diaphragm (pinhole) at the surface optically coupled to the focal surface of the objective. This principle is shown in Fig. 3.

The region that is responsible for a detected signal of a fluorescent marker (molecule) in the framework of the above-described optical system is usually called the confocal volume, which is ~1 fl (10^{-15} liter). But this definition of the confocal volume does not strictly determine its limits because isolation of the fluorescence signal from the noise can differ in efficiency. The size and shape of the confocal volume are determined by both characteristics of the focused exciting light and the system of the confocal recording of fluorescence. Moreover, parameters of the confocal volume depend on the properties of the sample (medium refractive index, photophysical features of the fluorophore) and also on the coverglass thickness and on other experimental conditions [50]. The confocal vol-

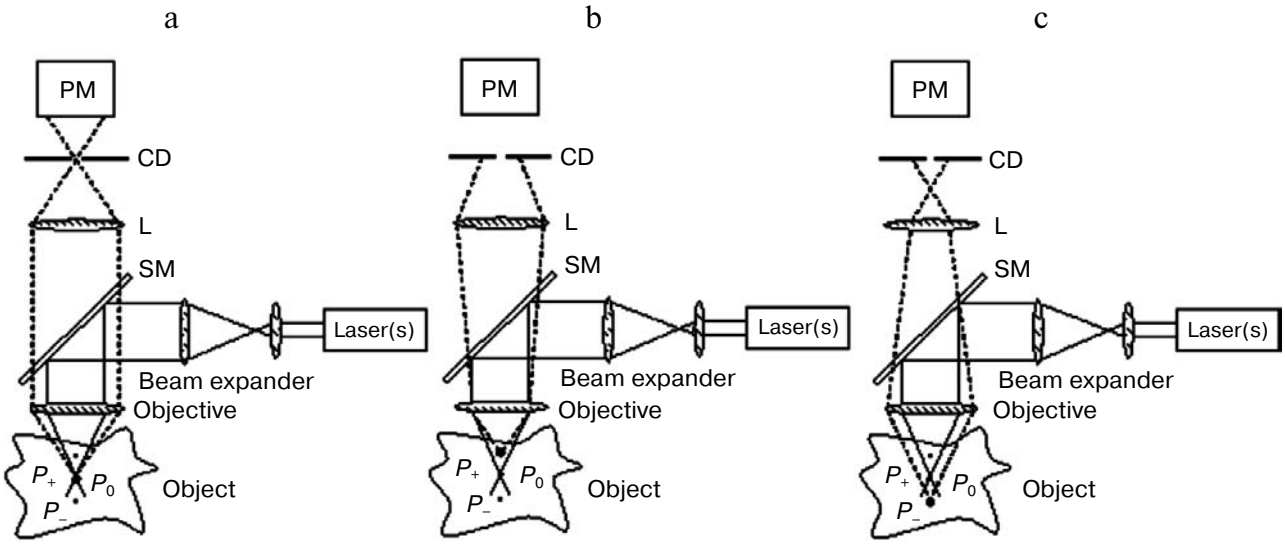

Fig. 3. Principle of confocal filtration of a signal. The laser beam (continuous line) is directed into the microscope objective with the selective mirror (SM) and is focused onto the point P_0 within the depth of the object under study. Fluorescence emitted from this point (dashed line) is collected with the objective and focused with the lens L at the conjugate focal surface of the objective on passing through a hole in the confocal diaphragm (CD) to the photoelectron multiplier (PM) (a). Fluorescence emitted from the points P_+ (b) and P_- (c) is defocused on the CD and does not reach the PM. This ensures suppression of the fluorescence emitted from the points of the sample located higher and lower than the focus of the objective.

ume is usually presented as an ellipsoid with r_0 and z_0 coordinates in the transversal and longitudinal direction, respectively (Fig. 4).

All these parameters influence the spatial function of the probability distribution of detecting a sample particle, which determines borders of the confocal volume. This function is often given as the Gaussian probability distribution, and in this case the confocal volume can be presented as an ellipsoid limited by size parameters z_0 and r_0, which are included in the Gaussian distribution. Moreover, a concept of the observation volume, or the effective volume, is also used, which is defined as the region in space where the probability of detecting the marker molecule is more than $1/e^2$ of the maximal level. In the case of the Gaussian distribution, the confocal volume size exceeds the effective volume size $2^{3/2}$-fold [51]:

$$V_{\text{conf}} = \left(\frac{\pi}{2}\right)^{3/2} r_0^2 z_0 = \left(\frac{1}{2}\right)^{3/2} V_{\text{ef}}. \quad (1)$$

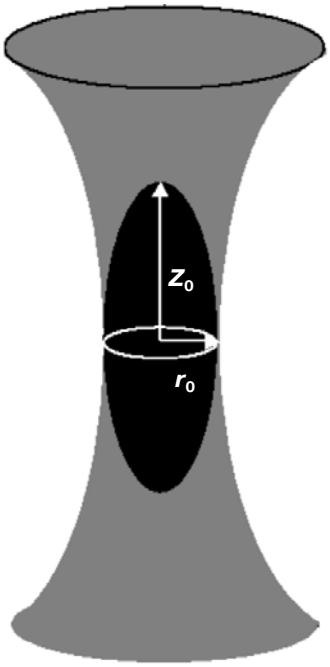

Fig. 4. Shape and parameters of the confocal volume (dark region).

There are the following main approaches for finding dimensions of the confocal volume [51]: measurement of a series of autocorrelation functions of diffusion of a fluorescent molecule in a solution with the known concentration; measurement of the autocorrelation function of diffusion of fluorescent molecules with the known diffusion coefficient; measurement of a signal of fluorescence intensity of fluorescent spheres (sphere dimensions are smaller than those of the confocal volume) fixed on the coverglass.

In the first approach the autocorrelation functions of diffusion of fluorescent dye molecules with known concentration are recorded in a series of dilutions. Then the effective volume is calculated by the formula:

$$V_{\text{ef}} = N/N_A c, \quad (2)$$

where N is the number of fluorescent molecules in the confocal volume, c is molar concentration of the substance, N_A is Avogadro's number.

An advantage of this approach is its independence of optical characteristics of the set-up and, consequently, it has no need for assumptions concerning the function of light distribution within the confocal volume. However, this approach is labor-consuming and requires samples to have definite photophysical properties. Conventional dyes including rhodamine 6G and sulforhodamine B cannot be used for calibrating the set-up by this approach because they are rapidly adsorbed onto the glass surface.

The other method is based on the hypothesis that the probability distribution of recording the particles within the confocal volume can be approximated with the Gaussian function in three-dimensional space. Then approximation of the experimental autocorrelation curve (see below) will allow us to determine the diffusion time τ_d of fluorescent molecules. If the diffusion coefficient of a substance is known, the size of the effective volume can be calculated by the formula:

$$V_{ef} = \pi^{3/2} k (4D\tau_d)^{3/2}, \quad (3)$$

where $k = z_0/r_0$.

The main advantage of this method is the rapid calibration. But accuracy of the determination depends on the accuracy of determination of the diffusion coefficient in water of the conventional fluorescent marker rhodamine 6G. In the literature values of this coefficient vary from 250 to 426 μm^2/sec at 22°C [39, 52-54].

Independently of the FCS methodology, the confocal volume can be determined by scanning a signal of the fluorescence intensity of fluorescent spheres fixed on a coverglass. The dimensions of these spheres must be lower than the geometric parameters of the confocal volume. Figure 5 shows such measurements for fluorescent spheres with diameter of 100 nm in three directions (y–x, z–x, and z–y) [51].

Autocorrelation function. The designation indicates that the correlation is assessed based on the finding of correlating (similar, associated) values during their determination within a certain time interval T. This is realized by comparing the signal intensity at moment t and $(t + \tau)$ over the whole period of recording the signal (Fig. 6). A strict determination of the autocorrelation function is given by Eq. (4):

$$G(\tau) = \frac{1}{T}\int_0^T F(t)F(t+\tau)dt = < F(t+\tau)F(t) >, \quad (4)$$

where $F(t)$ is a function of the fluorescence intensity depending on the time t.

In the literature a normalized autocorrelation function is often used resulting from division of Eq. (4) by the multiplier $<F(t)^2>$:

$$G(\tau) = \frac{<F(t)F(t+\tau)>}{<F(t)>^2}. \quad (5)$$

The normalized autocorrelation function takes values from zero to one.

For the function $G(\tau)$ analytical expressions have been obtained for cases of free movement of a particle within the three-dimensional space [29], a particle movement within the flow of a fluid [31, 55], a chemical reaction leading to changes in the particle brightness [11, 29]. For the case of three-dimensional diffusion the following expression is valid:

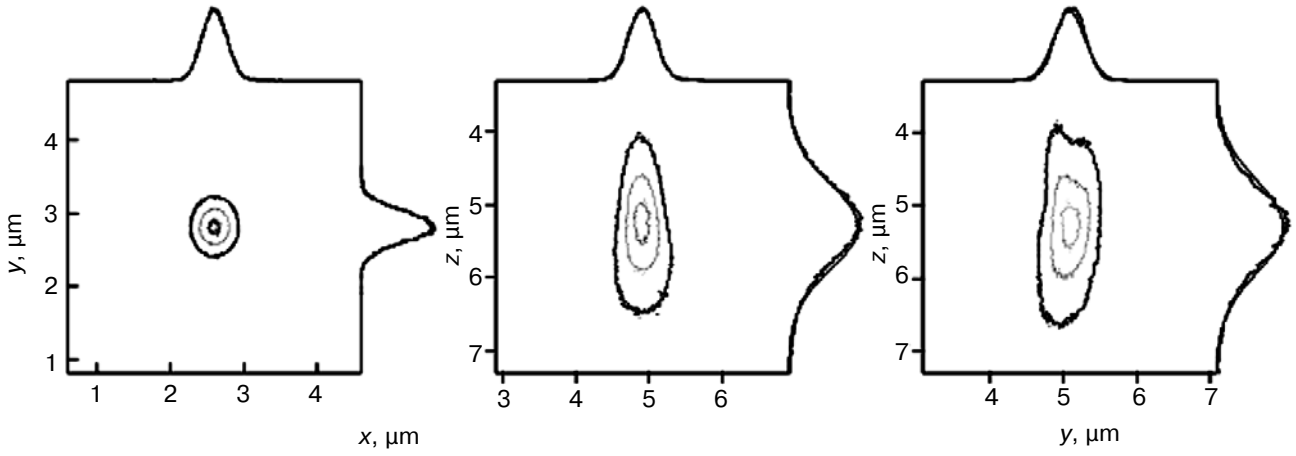

Fig. 5. Measurement of confocal volume dimensions by scanning the fluorescence intensity of immobile spheres. Gray outlines correspond to 90, 50, and 13.5% of the maximal fluorescence intensity. In the figure edges experimentally obtained borders of the confocal volume are shown in the corresponding surfaces (figure modified from work [51]).

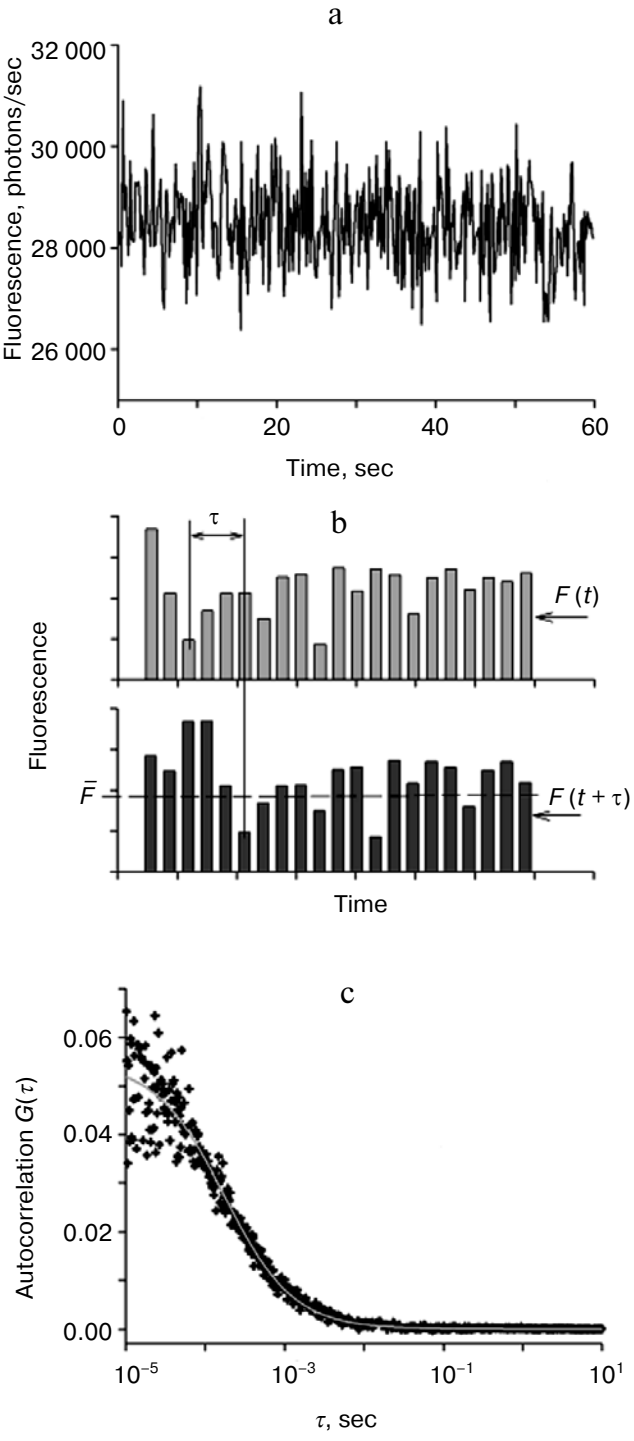

Fig. 6. Principle of autocorrelation treatment of fluorescence signal fluctuations. a) A typical time dependence of fluorescence of rhodamine 6G (R6G) at the excitation wavelength of 532 nm. b) Some data from panel (a) are shown on another time scale. The lower record is shifted by the time τ in relation to the upper record. $\bar{F}$ is the average level of the signal. To find the autocorrelation function at the given value of τ, it is necessary to summarize the product of values of the signals shown in these two records. c) The resulting autocorrelation function of the R6G fluorescence fluctuations (points) and its approximation by Eq. (6) (curve).

$$G(\tau) = \frac{1}{N}\left(\frac{1}{1+\frac{t}{\tau_d}}\right)\left(\frac{1}{\sqrt{1+\frac{r_0^2 \cdot t}{z_0^2 \cdot \tau_d}}}\right), \qquad (6)$$

where τ_d is the diffusion time, i.e. the dwell time of the particle inside the confocal volume before its exit due to free diffusion; N is the average number of particles inside the confocal volume; r_0, z_0 are geometrical parameters of the confocal volume.

The number of fluorophores within the confocal volume is inversely proportional to the autocorrelation function value in the limit of short time periods, i.e. at $\tau \to 0$ [29]:

$$G(\tau \to 0) = 1/N. \qquad (7)$$

This simple relation is valid not only for the case of Gaussian distribution of the probability of the particle being detected, but also in the general case for more complicated distributions. It follows from Eq. (7) that fluctuations in the fluorescence intensity damp on an increase in the number of particles within the confocal volume.

Histogram of fluorescence intensity distribution. The time dependence of fluorescence can be analyzed by calculating not only the autocorrelation function but also by using the distribution histogram of the fluorescence intensity, the photon counting histogram (PCH). According to its definition, this distribution corresponds to dependence of the incidence of a signal with the given value ($P(F)$) on the value itself, i.e. on F. The histogram shows the probability of presence within the confocal volume of molecules with a particular fluorescence intensity relative to the total number of recorded events. Thus, in contrast to the autocorrelation function, the PCH analyzes the distribution of fluorescence intensity of the particles that occur within the confocal volume during the observation time but not the mobility of these particles.

The main features of PCH can be explained in a simplified system when the confocal volume is a region of space with uniform probability of detecting a particle. In the case of particles with the same brightness, the probability of occurrence of N particles in the confocal volume is described by the Poisson distribution:

$$p(N) = \frac{\lambda^N e^{-\lambda}}{N!}, \qquad (8)$$

where λ is the average number of particles over the observation period. Due to the above-adopted condition of uniform probability of detecting the particle within a definite volume, PCH has also to have Poisson distribution. However, a nonuniform distribution of the proba-

bility of detecting the particle, as well as a random trajectory of the particle movement within the confocal volume cause distortions in the intensity distribution histogram that results in noticeable deviations from Poisson distribution.

For the case of two-photon excitation when the distribution of the particle detection can be well described by a Gaussian function, mathematical algorithms were derived to find a function for approximating experimental histograms, and this approach was tested in some experiments [48, 56-58]. It was shown that this approach could assess the brightness of a particle even in a system containing other particles with similar diffusion coefficients but with different brightness [47, 49, 59]. But, as it has been said earlier, two-photon excitation set-ups are still rarities. Therefore, we do not discuss in detail publications concerning PCH analysis on two-photon excitation.

However, let us analyze a key work to obtain an idea about possibilities of this type of FCS. This approach was used to determine stoichiometry of the binding of a fluorescently labeled ligand of a retinoid X-receptor located in the nuclear membrane of cells [60]. A series of control measurements were performed *in vitro* and *in vivo* to calculate the brightness dependence of a fluorescent marker molecule GFP on concentration of the preparation. Over a wide concentration range the luminosity of the single fluorophore molecule was constant in both solution and in nuclear membrane being ~4000 photon/sec per molecule. In the case of a heterogeneous system (monomer/ dimer) the recorded value of the particle brightness (ε_{app}) will be intermediate between the brightness values of the monomeric (ε_1) and dimeric (ε_2) forms, and the contribution of each of these complexes to the total brightness will depend on the numbers of, respectively, monomeric (N_1) and dimeric (N_2) particles by the equation:

$$\varepsilon_{app} = \frac{\varepsilon_1^2 N_1 + \varepsilon_2^2 N_2}{\varepsilon_1 N_1 + \varepsilon_2 N_2} . \quad (9)$$

COS strain cells were transfected with subsequent expression in them of GFP-labeled ligand for the retinoid X-receptor of the nuclear membrane. Increasing the ligand concentration increased the brightness of the ligand–receptor complex, which suggested oligomerization of the receptor. However, the value of the complex brightness was intermediate between the corresponding values for the monomeric and dimeric GFP forms, and the authors explained this to be caused by the low concentration insufficient for complete dimerization of the receptor. The addition to the cells of an activator of the receptor, 9-*cis*-retinoic acid, induced a rapid dimerization that was in a good agreement with the *in vitro* data for this receptor [61].

APPLICATIONS OF FLUORESCENCE CORRELATION SPECTROSCOPY

Studies of interaction and aggregation of biologically active molecules. Determination of mobility (diffusion coefficient) of fluorescent particles represented by fluorescently labeled biopolymers is the most common application of FCS in biology. Because the diffusion time τ_d is inversely proportional to the diffusion coefficient,

$$\tau_d = \frac{r_0^2}{4D} , \quad (10)$$

and, consequently, is directly proportional to the particle size,

$$D = \frac{kT}{6\pi\eta R} , \quad (11)$$

(k is the Boltzmann constant, T is temperature, η is viscosity of the solution, R is the particle radius), this parameter will change on aggregation of molecules under study or on formation of complexes with other polymers. The determination of τ_d was used for studies of protein–protein, protein–lipid, and ligand–receptor interactions, and also of aggregation of biomolecules under the influence of different factors. Studies of such interactions include analysis of autocorrelation functions of fluorescence fluctuations of a free fluorescent ligand, which as a rule has a small size, and of this ligand in complex with biomolecules (Fig. 7).

Aggregation of amphipathic biopolymers capable of producing micelles in aqueous solution is studied using lipophilic dyes, e.g. octadecyl rhodamine B (R18), which can be accumulated in the micelles. Analysis of autocorrelation functions resulted in determination of the aggregation number (N) of a lipopolysaccharide (LPS: *E. coli* 0111:B4) in aqueous solution [62]:

$$N = \frac{[\mathrm{LPS}] - \mathrm{cmc}}{[\mathrm{Mic}]} , \quad (12)$$

where cmc is the critical concentration of micelle production, [LPS] is the lipopolysaccharide total concentration, and [Mic] is the concentration of micelles.

Based on measurements of amplitude of the R18 autocorrelation function, the number of micelles was calculated within the confocal volume $N_{p,lim}$, and then the micelle concentration in aqueous solution was calculated using the formula:

$$[\mathrm{Mic}] = \frac{N_{p,lim}}{N_A V_f} , \quad (13)$$

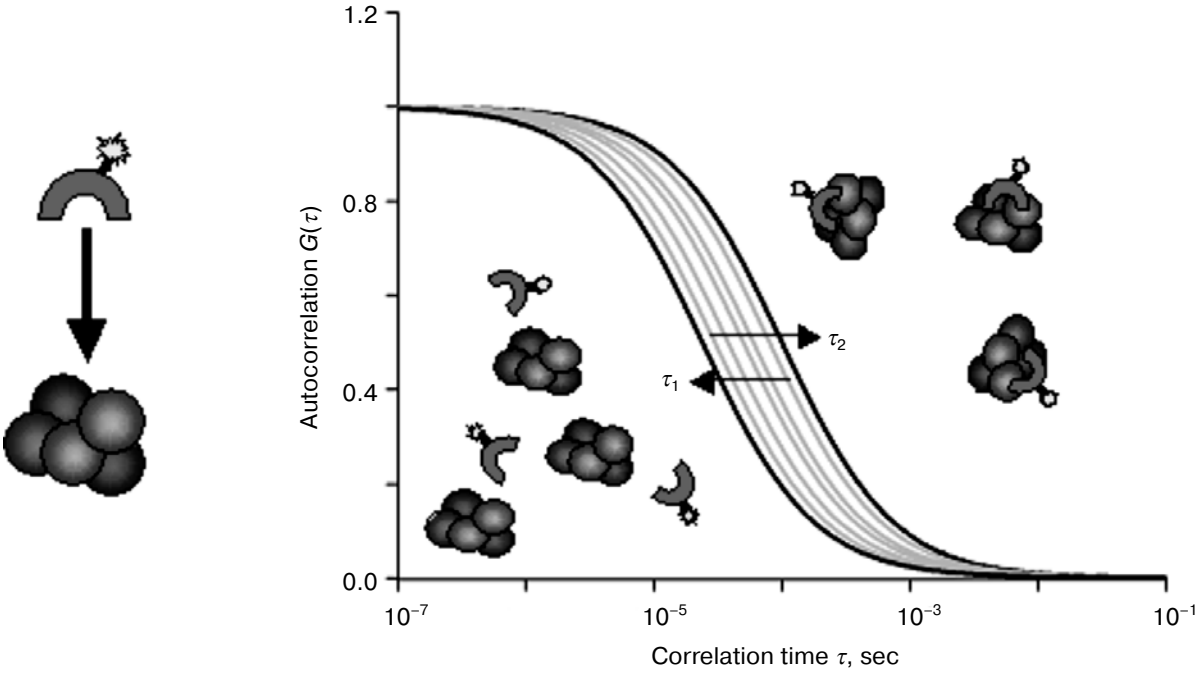

Fig. 7. Interaction of a fluorescently labeled ligand with a nonfluorescent partner resulting in a shift of the autocorrelation function to longer diffusion times τ_d due to formation of complexes and decrease in diffusion coefficient of the bound ligand.

where V_f is the confocal volume. The experimentally found value $N = 168 \pm 4$ was constant over a wide range of the lipopolysaccharide concentrations (0.7-150 μM).

Biopolymer aggregation can be recorded more directly by determination of the increase in diffusion time τ_d under conditions of covalently bound fluorescent label with the polymer under study. This approach was used to study β-amyloid protein aggregation in solution [63-65] and α-synuclein protein aggregation *in vitro* [66]. The α-synuclein aggregation plays a crucial role in Parkinson's disease, and mutant proteins found in the patients are more prone to aggregation than the wild type [67]. The authors found that proteins of the immunophilin family markedly accelerated aggregation of α-synuclein labeled with the dye Bodipy, which increases the diffusion time (τ_d) of labeled α-synuclein. The diffusion coefficient measured for the monomer was $(5.8 \pm 0.65)\cdot10^{-11}$ m^2/sec that on the calculation for the globular protein corresponded to the radius of 4.3 ± 0.5 nm. Upon termination of the aggregation, the diffusion time was two-three orders higher than at the beginning of the experiment. It is difficult to determine dimensions of such complexes based on data of the autocorrelation function because fluorescence fluctuations with a high amplitude significantly contribute to the form of the autocorrelation function. Due to the high sensitivity of FCS, concentrations of proteins to be determined by this method can be much lower than for similar measurements with the light scattering method.

Analysis of autocorrelation functions and measurement of diffusion coefficient combined with determination of the fluorescence anisotropy was also used to study the interaction with DNA of such proteins as a transcription activator NtrC [68] and 7-aminoactinomycin D [23]. In addition to the high sensitivity, this approach makes it possible to make determinations over a wide range of values of pH, salt concentrations, and temperature. Dissociation constants of NtrC are shown to significantly depend on the buffer composition and are two orders different (0.014 and 5.8 nM) for 15 and 600 mM potassium acetate, respectively. It should be noted that the fluorescence anisotropy could be measured using an FCS setup, which in this case is used as a microfluorimeter [25]. This approach was used to determine the binding constants of 7-aminoactinomycin D with DNA [23].

Consider in more detail an approach for assessment of the binding of a labeled ligand with a receptor, the latter having a significantly lower diffusion coefficient. Such a system is exemplified by the interaction of labeled antigens with antibodies to them [69-71], of labeled oligonucleotides with DNA and RNA [72, 73], or of proteins with lipid vesicles [74-77]. The diffusion time τ_d and the particle concentration in the confocal volume N were already discussed as main parameters of the autocorrelation function. In the system consisting of molecules with different τ_d values, the contribution of each type of particles ($i = 1, 2, 3, ..., M$) to the autocorrelation function value will be expressed as follows:

$$G(\tau) = \sum_{i=1}^{M} q_i^2 N_i^2 G_i(\tau) / \left[\sum_{i=1}^{M} q_i N_i \right]^2 = \sum_{i=1}^{M} A_i g_i(\tau) , \quad (14)$$

where N_i is the average number of particles, q_i is the normalized intensity of fluorescence, and $G_i(\tau)$ is the autocorrelation function of component i [78]. In the case of a system consisting of two types of particles (e.g. a free fluorescently labeled protein P and a complex of this protein with liposomes V) the amplitudes of the autocorrelation functions can be represented as:

$$A_p = \frac{N_p}{(N_p + \alpha N_v)^2}, \quad A_v = \frac{(\alpha N_v)^2}{N'(N_p + \alpha N_v)^2} , \quad (15)$$

where N_p and N_v are the numbers of free protein and liposome particles, respectively, N' is the number of particles consisting of liposome complexes with the bound protein, and α is the average number of protein molecules per liposome.

Using this approach, constants of the protein binding with liposomes can be calculated:

$$\frac{[P]_{mem}}{[P]_{tot}} = \frac{K[L]_{acc}}{1 + K[L]_{acc}} , \quad (16)$$

where $[P]_{mem}$ is the bound protein concentration, $[P]_{tot}$ is the initial protein concentration, and $[L]_{acc}$ is the total lipid concentration. The total amount of protein does not change, i.e. $N_0 = \alpha N_v + N_p$. Then

$$\frac{[P]_{mem}}{[P]_{tot}} = \frac{\alpha N_v}{N_0} = \frac{N_0 - A_p N_0^2}{N_0} = 1 - A_p N_0 . \quad (17)$$

The A_p value can be calculated by approximation of experimental autocorrelation diffusion curves of a protein bound with liposomes using the two-component Eq. (14), and the N_0 value can be calculated by approximation of the autocorrelation function of a free fluorescent protein in solution using Eq. (6). This approach was used for determination of binding constants of a fragment of the protein MARCKS (myristoylated alanine-rich C-kinase substrate) with liposomes different in the lipid composition, and results of the measurements were compared with data obtained by the routine determination of binding of a radiolabeled protein with the subsequent centrifugation of complexes [74]. The data were in a good agreement. FCS was also used to determine the binding with liposomes of other important proteins [79-81] and also the binding of proteins with natural membranes [40].

Among the great variety of biologically active molecules with bright fluorescence, photosensitizers are especially interesting. Photosensitizers are compounds that on absorption of a light quantum can generate reactive oxygen species (singlet oxygen and free radicals) having a photodynamic effect [82]. Many studies have revealed that the binding with the cell plasma membrane is an important stage of biological action of photosensitizers [83]. FCS allows researchers to obtain quantitative information about the binding of photosensitizers with both artificial [84] and natural membranes [27, 85] and also to study mechanism of this binding. In particular, by FCS the interaction of the central metal atom in the phthalocyanine molecule with the phosphate group of phospholipid was shown to be an important factor for the binding of metallophthalocyanine photosensitizers with phospholipid membranes [84, 85].

In particular, FCS studies of ligand–receptor systems are exemplified by studies on the interaction of different fluorescent ligands with receptors attached to nonfluorescent artificial spheres with a diameter in the range of nanometers. This approach was used to study the interaction of estrogen β-receptors with a fluorescently labeled protein as a coactivator of these receptors (SRC-1) in the presence of 17-β-estradiol and tamoxifen [86]. Analysis of the autocorrelation functions of the free ligand and of the ligand–receptor–sphere complex allowed the authors to calculate the equilibrium dissociation constants.

FCS can be used not only to measure particle mobility in solution, emulsion, or suspension, but also to determine the two-dimensional diffusion of particles in artificial and natural cell membranes [18, 87, 88]. Thus, FCS was used for determination of diffusion coefficients of fluorescently labeled lipids in a lipid bilayer, and the effect of cholesterol on their movement within membranes of giant liposomes was studied [89, 90]. This system is also characterized by formation of lipid domains with different phase state that results in a significantly different mobility of lipids depending on their position within the liposome. Recording the FCS signal in different places of the membrane of an immobile lipid vesicle, the following values of diffusion coefficients for the lipophilic dye Dil-C_{20} were found: $D = 3 \cdot 10^{-8}$ cm^2/sec in a liquid phase and $D = 2 \cdot 10^{-9}$ cm^2/sec for a cholesterol-enriched phase. The resulting values are in good agreement with data obtained by the method of fluorescence recovery after photobleaching (FRAP).

FCS was also used to measure lipid and protein diffusion in plasma membranes of cells [91-93]. These works confirmed the earlier found anomalous diffusion in cell membranes associated with existence of membrane immobile subdomains, the so-called rafts, and also of cytoskeleton-associated structures [94].

The determination of particle diffusion in a membrane requires that the membrane be precisely located within the center of the confocal volume. An approach was proposed for optimization of such experiments by measurement of a series of autocorrelation functions at different positions of the confocal volume relatively to the

membrane surface (the z axis) [95, 96]. By approximating the dependence of τ_d on z of the proposed function the coefficient diffusion value can be found for a particle within the membrane with precision significantly higher than for a single determination of τ_d.

By now great experience has accumulated in the application of FCS to living systems. For example, the autocorrelation function of fluorescently labeled calmodulin (Alexa 488 calmodulin) in the HEK293 cell cytoplasm was shown to be significantly shifted to longer time values compared to the autocorrelation function of isolated calmodulin in aqueous solution and to be characterized by several diffusion components [17]. This seemed to be associated with the higher viscosity of the cytoplasm and with formation of protein complexes with different cell components leading to a decrease in the diffusion coefficient in the cytoplasm.

FCS combined with FRAP was used to study the movement of oligonucleotides in the nucleus of cultured rat myoblasts [97]. The diffusion coefficients were determined for fluorescently labeled oligodeoxythymidine and of oligodeoxyadenine with the length of 43 nucleotides [97]. By FCS the major fraction of the two oligonucleotides was shown to move in the nucleus with the diffusion coefficient of $4 \cdot 10^{-7}$ cm^2/sec that corresponded to the diffusion coefficient in aqueous solution. A large fraction of intranuclear oligodeoxythymidine (45%) was also recorded which, as discriminated from oligodeoxyadenine, gave another slow component with diffusion coefficient $\leq 1 \cdot 10^{-7}$ cm^2/sec. Later, this slow component was shown to correspond to a complex of oligodeoxythymidine with polyadenine of intranuclear RNA. The two separate components were not detected by the FRAP method, and the diffusion coefficient value in this case was intermediate between the similar values for the fast and slow components measured by FCS. In the case of oligodeoxyadenine the diffusion coefficient values measured by the two methods were in good agreement.

FCS is actively used to study the interaction of ligands with receptors on natural membranes. Thus, the interaction of fluorescently labeled proinsulin C on plasma membrane receptors was studied on some human cell strains [40]. The affinity constants were found to be in the range of tenths of nanomoles depending on the cell type. The interaction was shown to be specific by suppressing the binding with specific inhibitors. Later, the interaction of the fibroblast growth factor receptors (Fgfr1 and Fgfr4) with their ligand Fgf8 in *Danio rerio* cells was studied *in vivo* [98]. This was done by introduction into the cells during embryogenesis of mRNAs of the corresponding proteins conjugated with the fluorescent proteins. The diffusion coefficients of the Fgfr receptors under study were determined in the plasma membrane, as well as constants of their affinity to Fgf8. Studies on ligand/receptor complexes in the cells using FCS were recently considered in a detailed review [16].

FCS was also used for diagnostics of different diseases, including HIV-infection and tuberculosis [99, 100]. On identification of HIV-infection, FCS was combined with an isothermal amplification of DNA/RNA, which allows selectively increasing the concentration of HIV-1 RNA. To synthesize DNA from the RNA template under analysis, a fluorescently labeled oligonucleotide primer was used specific to a region of the HIV-1 *gag* gene. The specific hybridization and elongation of the DNA chain due to the amplification resulted in an increase in the diffusion time of the fluorescently labeled molecule that was recorded by FCS. Such a modification of the isothermal amplification of DNA/RNA has some advantages. First, the process is monitored in real time by an increase in the diffusion time of the fluorescent molecule. Second, the process can be analyzed simultaneously in a large number of samples under study. Third, reaction systems need not be opened, which prevents the risk of contamination. To study the amplification kinetics of the *Mycobacterium tuberculosis* genomic DNA, the polymerase chain reaction was used instead of the isothermal amplification of DNA/RNA [100].

An interesting modification of FCS is a simultaneous measurement of fluorescence of two independent dyes (so-called two-color FCS) [101]. This allows researchers very accurately measure hybridization of oligonucleotides carrying two different fluorescent labels. The appearance of a cross-correlation signal indicates the formation of a complex between two nucleotides. Note that this approach does not require energy transfer from one dye to another, and this is its essential difference from fluorescence resonance energy transfer (FRET), which is also frequently used for detecting formation of intermolecular complexes and intramolecular interactions. In this case the cross-correlation signal indicates a simultaneous appearance of two labels within the confocal volume.

Using FCS for studies on kinetics of chemical reactions of biologically active molecules. In their first presentation of the FCS approach Magde et al. [28] demonstrated the possibility of studying kinetics of chemical reactions of biomolecules, in particular, the interaction of DNA with ethidium bromide. Consider in more detail the theory of FCS as applied to the monomolecular reaction of isomerization [11]:

$$A \underset{k_{BA}}{\overset{k_{AB}}{\longleftrightarrow}} B .$$

Assume that the A state of the substance is fluorescent and the B state is not fluorescent (fluorescence quantum yields are $Q_A = Q$, $Q_B = 0$) and that the diffusion coefficients do not change during the isomerization ($D_A = D_B = D$). Then the A and B concentrations will change due to diffusion processes and to the chemical reaction:

$$\frac{\partial \delta C_A(\vec{r},t)}{\partial t} = D\nabla^2 \delta C_A(\vec{r},t) - k_{AB}\delta C_A + k_{BA}\delta C_B , \quad (18)$$

$$\frac{\partial \delta C_B(\vec{r},t)}{\partial t} = D\nabla^2 \delta C_B(\vec{r},t) + k_{AB}\delta C_A - k_{BA}\delta C_B . \quad (19)$$

The solution of these equations [29] results in the following expression for the autocorrelation function:

$$G(\tau) = \frac{1}{N}\left(1+\frac{t}{\tau_d}\right)^{-1}\left(1+\frac{t}{\frac{z_0^2\tau_d}{r_0^2}}\right)^{-1/2}(1+K\exp(-\frac{t}{\tau_R})), \quad (20)$$

where $N = (C_A + C_B)V$ is the total number of A and B molecules within the volume under observation, $K = k_{AB}/k_{BA} = C_B/C_A$ is the equilibrium constant of the chemical reaction, and $\tau_R = (k_{AB} + k_{BA})^{-1}$ is the relaxation time of the chemical reaction.

Equation (20) contains two components, one of which is similar to that presented in Eq. (6) describing the autocorrelation function for three-dimensional diffusion, whereas the other corresponds to the contribution of chemical reaction. For the time interval $\tau << \tau_R, \tau_d$ amplitude of the autocorrelation function is inversely proportional to the number of fluorescent molecules A ($G(\tau\to0) = 1/N_A$, $N_A = C_A V_{conf}$). If the rate of the chemical reaction is higher than the diffusion time ($\tau_R << \tau_d$), then for time intervals longer than τ_R the autocorrelation function is mainly determined by diffusion (Eq. (6)), and in this case $G(\tau\to0) = 1/N$, i.e. the amplitude of the autocorrelation function depends on the total number of molecules that are associated with fast transitions between the A and B states.

The transition of a molecule from the fluorescent state into the nonfluorescent state can be associated with protonation/deprotonation of the molecule as has been observed for the case of green fluorescent protein (GFP) [102]. Analysis of the GFP autocorrelation functions at different pH values revealed that the transition time was 300 μsec at pH 7 and decreased to 45 μsec at pH 5, and 80% of molecules transited into the nonfluorescent state. At alkaline values of pH the transition time was 340 μsec and was not associated with protonation/deprotonation. The authors supposed that the flickering of protein fluorescence at pH 8-11 could be associated with an intramolecular transfer of a proton or with changes in the protein conformation.

In work [103] a simpler system was represented by transitions between the fluorescent and nonfluorescent states of the dye fluorescein in aqueous solution. In particular, the characteristic time for transition from the deprotonated doubly charged fluorescent form into the singly protonated anionic poorly fluorescent form at pH 9.4 was 5.4 μsec. In subsequent work of this laboratory FCS was used to study the lateral mobility of protons on the lipid membrane surface and the dissociation/binding of protons to the lipid surface [104]. This study was performed using two fluorescently labeled lipids based on phosphatidylethanolamine: one of them was conjugated with fluorescein and the other with Oregon Green. At pH > 8 protonation of the surface dye included the interaction of the proton with the total surface of the membrane (i.e. the membrane acted as a proton-collecting antenna), whereas at lower pH values the dye was protonated without involvement of the membrane, i.e. in the same way as in solution.

FCS was used to study kinetics of formation of potassium ion complexes with the fluorescently labeled K^+-indicator TAC-K^+ [105]. On formation of the indicator complex with potassium ions the free nonfluorescent indicator transited into a fluorescent state and bound with potassium ions:

$$\text{TAC} - \text{K}^+ \underset{k_a}{\overset{k_d}{\longleftrightarrow}} \text{TAC-K}^+,$$

where k_a is the complex formation constant and k_d is the complex decomposition constant. Analysis of autocorrelation functions at different concentrations of potassium ions in solution resulted in determination of the complex association and dissociation constants (0.0020 ± 0.0003 $mM^{-1}\cdot msec^{-1}$ and 0.12 ± 0.02 $msec^{-1}$, respectively).

FCS was used to study kinetics of interaction of pyronine Y and pyronine B with β-cyclodextrin [106]. On addition of cyclodextrin the autocorrelation function was shifted to longer times (from 250 to 400 μsec) and a fast component $G(\tau)$ appeared within the range of 0.1-1 μsec. The binding of both dyes was fast and limited by diffusion. The difference between their equilibrium binding constants was mainly contributed by the difference in the dissociation of the complex. Diffusion coefficients of the free dyes and their complexes with cyclodextrins were also determined.

FCS allows researchers to follow the formation of hydrogen bonds leading to the folding of biopolymers. Thus, FCS was used to study kinetics of loop formation in a short-chain DNA molecule [107]. A fluorescent dye (rhodamine 6G) was covalently attached to one end of the DNA molecule and the quencher of rhodamine fluorescence DABCYL was bound to its other end. Thus, the fluorescence was bright in the unfolded state of DNA and significantly quenched for hairpin formation. Equation (20) was transformed for the two-dimensional movement and used for calculation of kinetic parameters of a chemical reaction resulting in production of secondary structure of DNA:

$$G(\tau) = \frac{1}{N}\left(\frac{1}{1+\frac{t}{\tau_d}}\right)\left(1+\frac{1-p}{p}\exp^{-\frac{t}{\tau_R}}\right), \quad (21)$$

where p is the fraction of unfolded molecules, $1/\tau_R = k\_ + k_+$, $k\_$ is the rate constant of transition from the closed

(folded) state to the open state, k_+ is the rate constant of transition from the free state to the folded state. Because the diffusion time of the DNA molecule (τ_d = 150 μsec) occurred within the time range of the reaction τ_R = 5 μsec-1 msec, the control specimen of DNA lacking the quencher of the rhodamine 6G fluorescence was studied to calculate τ_R, i.e. the autocorrelation function characterizing only the diffusion component. For a DNA fragment consisting of 21 nucleotides τ_R = 134 μsec at 10°C and τ_R = 28 μsec at 45°C.

FCS was used to study a similar system, but instead of fluorescence quenching the energy transfer was determined from one end of RNA molecule to the other (FRET) [108]. This study was performed using a pair of dyes, Cy3 and Cy5. The conformation dynamics of RNA led to appearance of fluctuations in the FRET signal within the millisecond range, and these fluctuations depended on concentrations of magnesium and sodium ions. The authors concluded that the association/dissociation of ions did not contribute to the observed intramolecular changes in the RNA molecule. Note that in this work RNA molecules were immobilized on a streptavidin-coated glass with an additionally attached biotin molecule.

In work [109] FCS was used to study a superhelix formation of a 2686-bp plasmid DNA (plasmid pUC18). In this case fluorescence of the plasmid labeled with rhodamine 6G by one base was caused by conformational dynamics of this elongated molecule with spatial dimensions exceeding those of the confocal volume. The circular DNA could be circle-shaped and also form helices and additional loops. The autocorrelation function of loop-free DNA could be sufficiently described by a simple equation of diffusion, and the presence of loops led to appearance of an additional component $G(\tau)$ which corresponded to fast transitions between different conformations of DNA.

FCS is used to study conformational dynamics not only of DNA but also of proteins. The autocorrelation function was measured for an intestinal fatty acid-binding protein, or to be more precise, of its cysteine mutant in position 60 with a covalently bound fluorescein Val60Flu [110]. Equation (6) describing the pure diffusion dynamics of particles does not adequately describe the $G(\tau)$ of the protein observed in solution. And the measured value of τ_d was only slightly over the τ_d value for free molecules of the dye (71 and 55 μsec, respectively). However, Eq. (20), which in addition to the diffusion component also includes the first order reaction characterizing conformational dynamics of the protein, described the $G(\tau)$ of the protein very precisely. And the τ_d value (120 μsec) determined for the protein under study already sufficiently corresponded to a particle with such a high molecular weight. The component involving the conformational dynamics τ_R (35 μsec) significantly depended on pH and disappeared on acidification, which was explained by denaturation of the studied protein. In work [111] a similar approach was used to study dynamics of a small protein subunit of oxoglutarate dehydrogenase from *E. coli*. A number of characteristic times were found for the folding of this protein, and the shortest time was 500 nsec. The authors noted that this time was shorter than had been predicted by the "stochastic ball" model of a biopolymer.

Using FCS for study of movement of individual molecules in flow systems. FCS can be used to determine rates of flows of fluorescently labeled particles, including biologically important molecules [55, 112-114]. The formula for the autocorrelation function in the case of particle movement in a flow with a certain rate is as follows [55]:

$$G(\tau) = \frac{1}{N} A \exp\left\{\left(\frac{t}{\tau_{flow}}\right)^2 A\right\} + 1, \qquad (22)$$

where

$$A = \left(1 + \frac{t}{\tau_d}\right)^{-1} \left(1 + \frac{r_0^2 t}{z_0^2 \tau_d}\right)^{-1/2}. \qquad (23)$$

In this equation τ_d and τ_{flow} are, respectively, times of the particle passage across the confocal volume due to free diffusion and under the influence of a constant flow of fluid. The τ_{flow} value can be used to determine the rate of the fluid flow:

$$V = \frac{r_0}{\tau_{flow}}, \qquad (24)$$

where r_0 is the confocal surface radius.

Virtually, the flow is usually varied by positioning the reservoir with a diluted solution of the fluorescently labeled preparation on a different height. The pressure drop creates a stationary flow with rate V proportional to the pressure difference. The flow rate is maximal in the center of the channel and approaches zero near its walls [55] in accordance with the parabolic profile of the rate in the channel section, which is given by the Poiseuille equation for laminar flow:

$$V(x) = \frac{\Delta p}{2\eta l}(d^2 - x^2), \qquad (25)$$

where η is the solution viscosity, l is the channel length, and d is the channel half-width. In work [55] uridine phosphate covalently labeled with tetramethylrhodamine (10^{-10} M) was used as a fluorescent marker for determination of the flow rate.

The FCS set-up equipped with a flow capillary is very like a flow cytofluorimeter and can be used for the

same purpose [115]. However, despite the external resemblance they are significantly different in the geometry of the focused exciting light. In the flow cytofluorimeter the exciting light spot is large and the brightness within the spot is more uniform, which results in a significantly lower luminescence than in FCS. Therefore, the flow cytofluorimeter is more appropriate to study whole colored cells because the brightness of isolated organelles of submicron size is usually insufficient. By contrast, FCS is sufficiently sensitive for recording luminescence of single molecules of a fluorophore.

Using the fluid flow in the experimental cell for increasing the number of recorded events of particle passage across the confocal volume was described in work [116] where fluorescently labeled single- and double-stranded DNA molecules were recorded [116]. Amplitudes of the fluorescence peaks were determined, and this promoted population analysis of DNA suspension at different temperatures. Width dependences of FCS signal peaks and of the area under the peaks on the flow rate and particle dimensions were analyzed [115]. The width and area of the peak were shown to increase with an increase in the particle dimensions at constant rate of flow. The authors proposed using this dependence for determination of dimensions of particles moving in a flow with a definite rate.

Mixing of preparations directly within the confocal volume using microfluidics creates new opportunities for studies on kinetics of fast interactions. Thus, a modified microcell was shown where two reacting preparations were separated by a buffer solution to locate the mixing only within the laser beam focus [117]. The cell had five entrances and one exit. Solution A with one type of molecules was injected into the central channel and solution B with another type of biomolecules was injected perpendicularly. Along the diagonal a flow of solution A without biomolecules was used to prevent untimely mixing of the preparations from solutions A and B. FCS allowed researchers to completely characterize conditions of the fluorescence quenching within such a cell and to assess the rate of mixing of the two solutions by quenching fluorescently labeled dextran under the influence of potassium iodide (the characteristic mixing time is 0.1 msec).

The more sophisticated FCS variant was specially elaborated to more completely characterize fluid flows. It is a dual-focus cross-correlation set-up, which provides for the determination not only of the flow rate but also the direction of the particle movement. The optical scheme in this case is fundamentally different from the scheme shown in Fig. 3 by the presence of two observation volumes with the distance between them of ~2 μm [112]. At each measurement two cross-correlation curves are recorded, which correspond to correlation of the fluorescence signals within the first and second confocal volumes in the flow direction and against it. The cross-correlation function of the movement in the flow direction has a peak corresponding to the same particle passage first across the first and then across the second confocal volume. If the flow is directed perpendicularly to the vector connecting the two confocal volumes, the signal cross-correlation will be absent [112].

FCS can be also used combined with capillary electrophoresis [118-121], which allows charged substances to be separated in electric field. Theoretically, to reliably discriminate two fluorescent substances using conventional FCS, they are to have no less than an eighth-fold difference in molecular weight M (because $D \sim M^{-1/3}$), whereas the electrophoretic mobility is proportional to the charge/weight ratio, i.e. is more sensitive to changes in the molecular weight [119]. However, changes in the mobility in an electric field of a series of DNA molecules revealed virtually absence of mobility dependence on length, whereas the diffusion coefficient measured by FCS noticeably changed in accordance with the model of a rigid cylinder [120].

Determination of blood flow rate in blood vessels is an important application of FCS in biological studies. The presence of autofluorescent blood components including erythrocytes makes it possible to perform studies without an additional modification of biomolecules or introduction of markers. Combined with the laser scanning microscopy, FCS was used for determination of blood flow rate in the brain vessels of embryo of the fish *D. rerio* [122]. To visualize the blood vessels, in this experiment GFP was expressed in all endothelial cells of the vessels. Upon fixation of the embryo, a single vessel was chosen for subsequent measurements of the flow rate by FCS. The resulting value of the rate (1.67 mm/sec) was in a good agreement with the values obtained for vessels of the *D. rerio* heart [123].

Analysis of fluorescence peaks in suspension of bright particles. The processing of a fluorescence signal as an autocorrelation function is not always optimal for analysis of a system using FCS. Thus, in the case of a mixture of particles significantly different in brightness, $G(\tau)$ will be virtually completely determined by a contribution of the bright particles. Moreover, in a suspension of large particles (liposomes, isolated mitochondria, etc.) in low concentrations the reproducible measurement of $G(\tau)$ is associated with accumulation of a signal over a long period (up to some hours) that makes the solution of this problem difficult. Therefore, another approach was proposed for analyzing such systems – to calculate the number and amplitude of the fluorescence peaks in the initial time record of the signal. This approach is very specific for analysis of electrophysiological data and has a sophisticated mathematical apparatus.

In particular, peaks were analyzed to study the binding of fluorescently labeled colchicine with tubulin [124, 125]. If a solution contains only fluorescent ligand molecules, the time dependence of the fluorescence signal will be a straight line with small deviations from the average

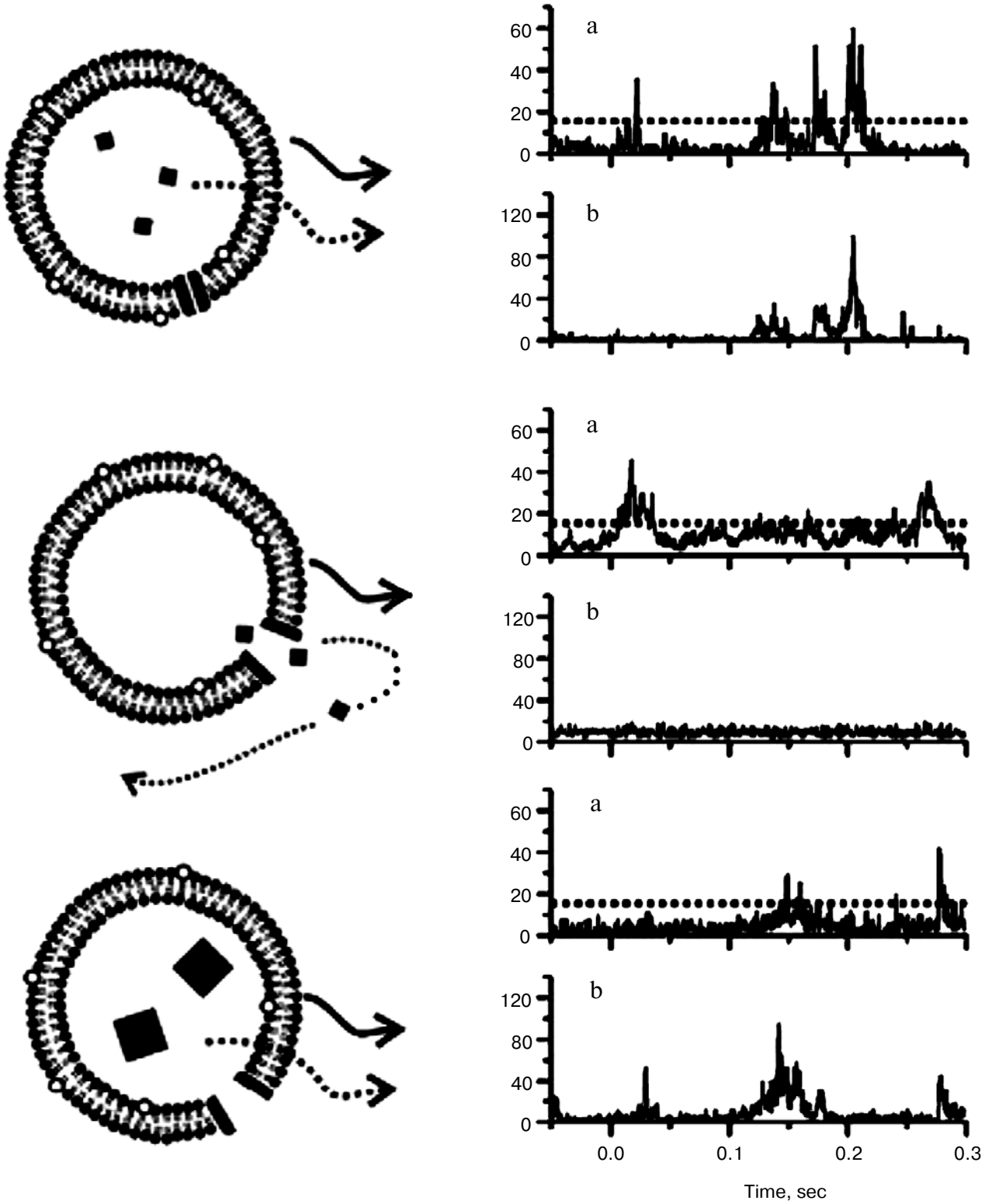

Fig. 8. Time dependences of fluorescence intensity of liposomes carrying two fluorescent markers: a) for lipophilic label; b) simultaneously measured dependence for hydrophilic label (figure modified from [129]).

value. The addition into the solution of particles capable of binding a number of the fluorescent ligand molecules is accompanied by appearance in the records of fluorescence intensity of peaks with a high amplitude specific for formation of complexes. Because the particles which have bound different numbers of fluorescent molecules are different in brightness, the authors propose to analyze not the number of complexes produced, i.e. the peaks, but the total area under the peaks in the plot of time dependence of the fluorescence intensity. Control measurements revealed a linear dependence of this parameter on the number of particles with the adsorbed fluorescent ligand [124]. This analysis is usually performed for determination of the ligand binding constant [124].

A similar approach was used to analyze the binding of the cationic polymer poly[(2-dimethylamino)ethylmethacrylate] (pDMAEMA) with a fluorescently labeled oligonucleotide (Rh-ON) [126]. Complexes of DNA with cationic polymers are known to be more effective in transfection than free DNA. The composition of pDMAEMA–Rh-ON complexes was studied as a function of the ratio of cation and anion charges φ(+/–). The authors found that in the complexes of a cationic polymer with oligonucleotide for which $\varphi < 1$ the fluorescence was quenched due to a high concentration of the oligonucleotide on one chain of the polymer. Further increase in the polymer concentration resulted in an increase in the number of high amplitude peaks that was associated with the distribution of the oligonucleotide molecules between the polymer chains in the concentration insufficient for autoquenching. Upon reaching a certain ratio of the charges when each chain of the polymer had one corresponding molecule of the oligonucleotide, the further increase in the polymer concentration would not lead to an increase in the number of peaks. Just this was observed by the authors at $\varphi = 15$ [126]. The same approach was used to study the binding of other cationic polymers [127].

A similar variant of FCS, which included analysis of fluorescence peaks, was also used to study leakage of a fluorescent dye from closed lipid vesicles (liposomes) under the influence of different factors [128-132]. Van den Bogaart et al. [129, 133] used a modified analysis of peaks, which included recording of signals of two fluorescent markers with different spectral properties. The authors called their modification dual-color fluorescence-burst analysis (DCFBA). One hydrophilic marker was inside the liposomes, whereas the other marker was lipophilic and located within the lipid bilayer. If the treatment did not result in formation of pores in the membrane and the integrity of liposomes was retained, the fluorescence intensity signals of the two markers were coincident in time and duration because both markers moved together in each liposome. If a channel-forming agent was added to the liposomes and dimensions of the formed pores were larger than those of the hydrophilic marker molecules, this marker left the liposomes and the fluorescence signals ceased to coincide (Fig. 8).

Analysis of the peaks resulted in determination of the concentration of marker molecules inside liposomes, which was calculated by the following formula for each peak:

$$C_i = \frac{\int_{t_1}^{t_2} I_{\text{size-marker}}\, dt}{\left(\int_{t_1}^{t_2} I_{\text{liposome}}\, dt\right)^{\frac{3}{2}}}, \qquad (26)$$

where I_{liposome} and $I_{\text{size-marker}}$ are, respectively, the fluorescence signal of liposomes and of molecules of inner markers, and the I_{liposome} value is greater than a certain value I_{offset} in the time interval t_1-t_2; the degree 3/2 in the denominator is associated with location of the fluorescent label on the surface of liposomes, whereas marker molecules are in the solution within the liposomes.

This approach was used to study a mechanosensitive channel MscL [133]. This protein was incorporated into liposomes colored with the lipophilic label DiO and loaded with fluorescently labeled molecules of different size. For compounds with size of 2-3 nm (proteins with molecular weight below 7 kDa) the concentration of marker molecules inside the liposomes decreased with the opening of the MscL channel. Results of studies on single liposomes using DCFBA were used for assessment of the incorporation of MscL protein into liposomes. Only 50% of all liposomes loose their contents on the channel activation. This means that about a half of the liposomes carried inactive protein. Based on the protein/lipid ratio, it was calculated that one liposome includes ~10 protein molecules that form channels. The incorporation efficiency in this case was <10%.

This approach can be very effective also in studies of ligand/receptor systems. For such studies it is necessary to prepare liposomes with an incorporated fluorescently labeled protein, and the ligand also has to carry a fluorescent label with a spectrum different from that of the receptor label. And the ligand affinity for the receptor must be sufficiently high to exclude the background signal of fluorescence of the free ligand in solution. This approach was used for calculation of the binding constant of the fluorescently labeled protein SecA with the fluorescently labeled protein of the SecYEG channel of the secretion system of *E. coli*. By changing concentration of the unlabeled ligand (SecA) the binding constant $K_{\text{ass}} =$ 4 nM was obtained [129, 134].

The possibility of using a flow capillary for analyzing peaks of the fluorescence signal was considered earlier. An alternative approach is a stirring of a solution of suspension of particles. In our laboratory peaks of the fluorescence signal were analyzed to study the binding of potential-dependent dyes with isolated mitochondria [26, 135]. Mitochondria are significantly larger than lipo-

somes; therefore, analysis of $G(\tau)$ is difficult or even impossible because of instability of isolated mitochondria. The analysis of peaks was significantly improved by stirring the mitochondrial suspension. Figure 9 presents some records of fluorescence of tetramethylrhodamine ethyl ether (TMRE) in a mitochondrial suspension without stirring (left side) and under conditions of stirring (right side). Peaks of TMRE fluorescence are manifested most distinctly in the middle record performed under conditions of energization of the mitochondria. De-energization is associated with a decrease in the membrane potential leading to exit of the cationic dye into the medium (lower records in Fig. 9). This approach can be used to analyze binding with mitochondria not only of hydrophobic compounds but also of such relatively hydrophilic substances as fluorescently labeled ATP [136] and of different charged phthalocyanines [85].

It should be noted that the stirring of a suspension of particles to increase the number of recorded events could be replaced by translocation of the confocal volume within the cell. This can be realized either by a synchronized movement of the laser beam and of the confocal diaphragm (as it takes place in a confocal microscope) or by shifting the microscope table. This modification of FCS was realized as early as at the dawn of the development of the method [137] and was successfully used to

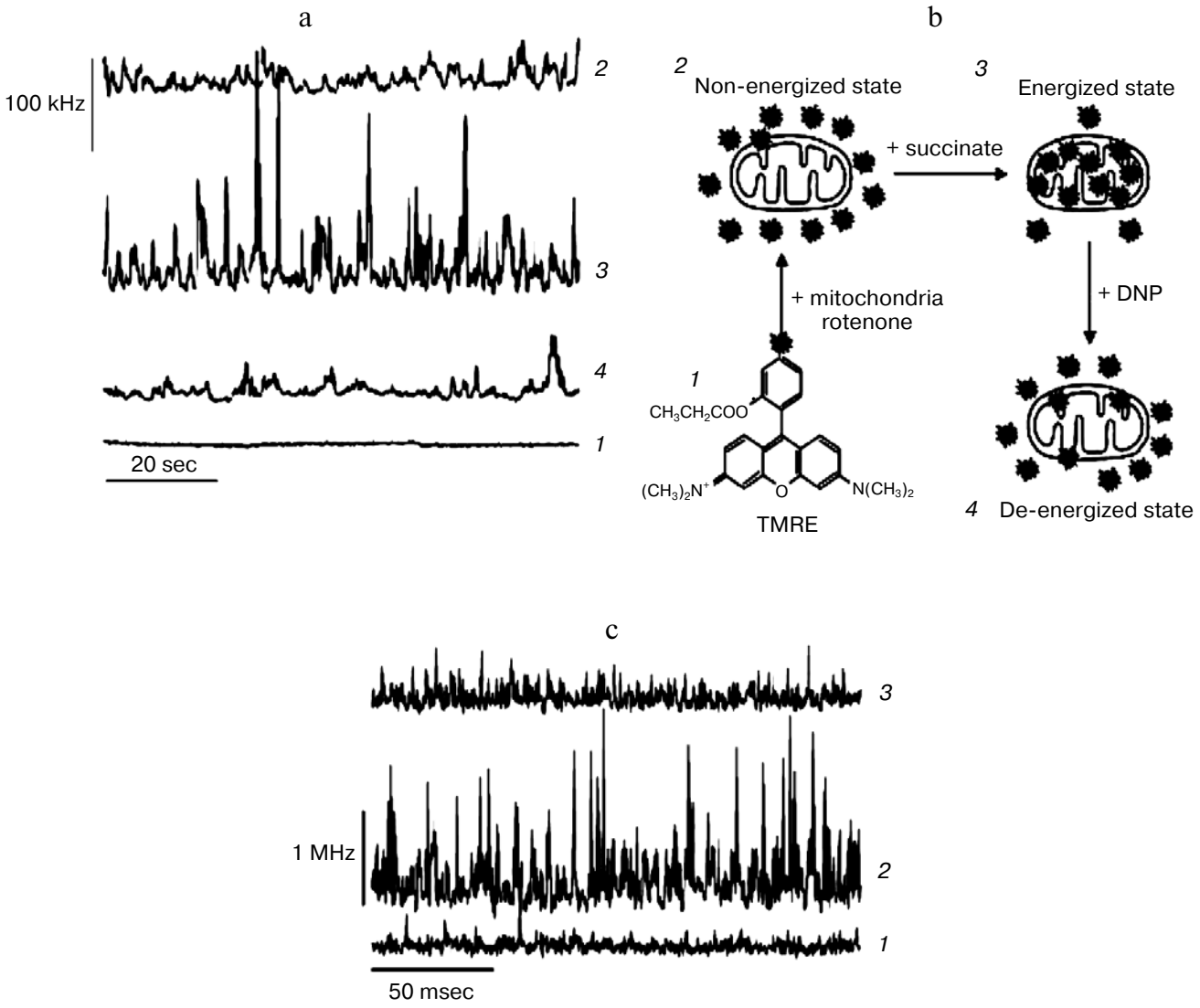

Fig. 9. a) Time dependence of fluorescence intensity for suspension of mitochondria stained with TMRE (0.3 μM) without stirring: *1*) control record in TMRE solution; *2*) non-energized state of mitochondria in the presence of rotenone; *3*) energized state of mitochondria upon addition of succinate; *4*) de-energized state of mitochondria upon addition of DNP. b) Scheme of succession of events during interaction of the dye TMRE with an individual mitochondrion in different energetic states. c) Time dependence of fluorescence intensity for suspension of mitochondria colored with TMRE (0.03 μM) under conditions of stirring: *1*) mitochondria and rotenone; *2*) addition of succinate; *3*) addition of DNP.

study oligomerization of proteins in solution [138], recording trajectories of nanoparticle movements [139], and also to study protein dynamics and ligand/receptor interactions in living cells [19].

The considered applications of the FCS method comprise various fields of investigation, from simple chemical systems (solution/micelle) to fine regulation processes at the level of living cells. Applications concerning artificial and natural membranes are presented in the review most completely. This is associated with the sphere of primary scientific interests of the authors of the review. Nevertheless, we tried to describe also the most specific examples of other applications. Our major purpose was to show by these examples broad possibilities of the method and allow readers to assess its usefulness for studies of specific problems.

FCS is characterized by a high sensitivity which makes it possible to work at concentrations of a fluorescent marker equal to ~1 nM in volumes from 10 to 1000 μl, i.e. a typical measurement requires ~10^{-13} mole of a substance. However, FCS cannot be considered as a direct approach for measurement of fluorescence of single molecules, because within the typical period of measurements (1 min) statistics are analyzed for a great ensemble of molecules (typically ~10^3 molecules), which allows researchers to average both the features of the marker itself (brightness, mobility, etc.) and parameters of its interaction with other components of the system. Consequently, this method cannot be used to directly solve problems typical for recording single molecules, e.g. fluorescence blinking and identification of multiple intermediates of reactions, including different conformational states in forward and back reaction pathways [140-144]. Thus, FCS is in a halfway of studies on integral properties of a substance as a whole and on individual properties of isolated molecules with all consequent advantages and shortcomings.

The sensitivity of FCS can be characterized by comparing studies on the interaction of labeled oligonucleotides with DNA. The sensitivity of FCS approximately corresponds to the sensitivity of measurements of interactions with a radioactive label, but FCS does not require operations with radioactivity and physical separation of the components. For FCS a significantly smaller amount of a substance is required as compared with measurements using circular dichroism or calorimetric methods. Moreover, FCS gives additional information about diffusion coefficients, brightness of particles, degree of their aggregation, concentration of complexes, and, finally, about kinetics of intermolecular and intramolecular interactions [12].

If the present review has provoked the reader interest associated with a specific use of this approach, a question arises how to realize it. In other words, is it difficult to make such a set-up in the laboratory? Our experience has shown that the set-up can be made if the corresponding blocks are present. The main blocks are a fluorescence microscope, laser, photoelectric multiplier (PM) (or a highly sensitive photodiode), and a correlator. A laser, PM, and correlator are standard components of a rather widely distributed apparatus for measurement of dynamic light scattering. Moreover, in contrast to gas lasers, modern solid-state lasers (especially a green one) are already used rather widely and have been working continuously for a long time. Adjusting an FCS set-up built with the above-listed blocks is described in the literature in detail [11, 13]. Our own experience has shown that even in the absence of practice in working with optical instruments, the adjustment of a self-made FCS set-up takes only a few days. Note also that companies producing confocal microscopes started to produce apparatuses for FCS. The authors will think their challenge accomplished if this review proves to the readers that it is necessary to construct an FCS set-up (or to buy it) and to use it in their experimental work. No doubt, FCS has to occupy a more significant place in modern Russian science.

The authors are grateful to Prof. D. B. Zorov (Belozersky Institute of Physico-Chemical Biology, Lomonosov Moscow State University) for fruitful discussion of the review and to Prof. Petra Schwille (Dresden Technical University) for providing us with models of some figures.

REFERENCES

1. Kask, P., and Kyandler, T. (1978) *Izv. AN ESSR*, **27**, 73-78.
2. Kask, P., Kyandler, T., Sirk, A., Karu, T., and Lippmaa, E. (1979) *Izv. AN ESSR*, **28**, 221-226.
3. Kyandler, T., Kask, P., Piksarv, P., Sirk, A., and Lippmaa, E. (1982) *Izv. AN ESSR*, **31**, 314-319.
4. Kyandler, T. E. (1985) *Fluorescence Correlation Spectroscopy in Studies on Dynamics of Chemical Systems*: Candidate's dissertation [in Russian], Tartu State University, Tartu.
5. Kask, P., Piksarv, P., Mets, U., Pooga, M., and Lippmaa, E. (1987) *Eur. Biophys. J.*, **14**, 257-261.
6. Kask, P., Piksarv, P., Pooga, M., Mets, U., and Lippmaa, E. (1989) *Biophys. J.*, **55**, 213-220.
7. Kask, P. (1987) *Stud. Biophys.*, **118**, 7-24.
8. Rigler, R., and Elson, E. (eds.) (2001) *Fluorescence Correlation Spectroscopy: Theory and Applications*, Springer, N. Y.
9. Eigen, M., and Rigler, R. (1994) *Proc. Natl. Acad. Sci. USA*, **91**, 5740-5747.
10. Schwille, P. (2001) *Cell. Biochem. Biophys.*, **34**, 383-408.
11. Krichevsky, O., and Bonnet, G. (2002) *Rep. Prog. Phys.*, **65**, 251-297.
12. Hess, S. T., Huang, S., Heikal, A. A., and Webb, W. W. (2002) *Biochemistry*, **41**, 697-705.
13. Sengupta, P., Balaji, J., and Maiti, S. (2002) *Methods*, **27**, 374-387.
14. Enderlein, J., Gregor, I., Patra, D., and Fitter, J. (2004) *Curr. Pharm. Biotechnol.*, **5**, 155-161.

15. Gosch, M., and Rigler, R. (2005) *Adv. Drug Deliv. Rev.*, **57**, 169-190.
16. Briddon, S. J., and Hill, S. J. (2007) *Trends Pharmacol. Sci.*, **28**, 637-645.
17. Kim, S. A., Heinze, K. G., and Schwille, P. (2007) *Nat. Methods*, **4**, 963-973.
18. Machan, R., and Hof, M. (2010) *Biochim. Biophys. Acta*, **1798**, 1377-1391.
19. Petrasek, Z., Ries, J., and Schwille, P. (2010) *Meth. Enzymol.*, **472**, 317-343.
20. Garcia-Saez, A. J., and Schwille, P. (2010) *Biochim. Biophys. Acta*, **1798**, 766-776.
21. Serdyuk, I. N., Zaccai, N. R., and Zaccai, J. (2007) in *Methods in Molecular Biophysics: Structure, Dynamics, Function*, Cambridge University Press, Cambridge.
22. Sukharev, V. I., and Vekshin, N. L. (2000) *Bioorg. Khim.*, **26**, 723-727.
23. Kovalev, A. E., Yakovenko, A. A., and Vekshin, N. L. (2004) *Biofizika*, **49**, 1030-1037.
24. Tatarkova, S. A., Lloid, K., Hara, S. K., and Berk, D. (2003) *Kvant. Elektron.*, **33**, 357-362.
25. Vekshin, N. L. (2006) *Fluorescence Spectroscopy of Biopolymers* [in Russian], Foton-Vek, Pushchino.
26. Perevoshchikova, I. V., Sorochkina, A. I., Zorov, D. B., and Antonenko, Yu. N. (2009) *Biochemistry (Moscow)*, **74**, 663-671.
27. Strakhovskaya, M. G., Antonenko, Yu. N., Pashkovskaya, A. A., Kotova, E. A., Kireev, V., Zhukhovitsky, V. G., Kuznetsova, N. A., Yuzhakova, O. A., Negrimovsky, V. M., and Rubin, A. B. (2009) *Biochemistry (Moscow)*, **74**, 1305-1314.
28. Magde, D., Elson, E. L., and Webb, W. W. (1972) *Phys. Rev. Lett.*, **29**, 705-708.
29. Elson, E. L., and Magde, D. (1974) *Biopolymers*, **13**, 1-27.
30. Magde, D., Elson, E. L., and Webb, W. W. (1974) *Biopolymers*, **13**, 29-61.
31. Magde, D., Webb, W. W., and Elson, E. L. (1978) *Biopolymers*, **17**, 361-376.
32. Ehrenberg, M., and Rigler, R. (1974) *Chem. Phys.*, **4**, 390-401.
33. Ehrenberg, M., and Rigler, R. (1976) *Q. Rev. Biophys.*, **9**, 69-81.
34. Aragon, S. R., and Pecora, R. (1975) *Biopolymers*, **14**, 119-138.
35. Koppel, D. E., Axelrod, D., Schlessinger, J., Elson, E. L., and Webb, W. W. (1976) *Biophys. J.*, **16**, 1315-1329.
36. Aragon, S. R., and Pecora, R. (1976) *J. Chem. Phys.*, **64**, 1791-1803.
37. Webb, W. W. (1976) *Q. Rev. Biophys.*, **9**, 49-68.
38. Fahey, P. F., Koppel, D. E., Barak, L. S., Wolf, D. E., Elson, E. L., and Webb, W. W. (1977) *Science*, **195**, 305-306.
39. Rigler, R., Mets, U., Widengren, J., and Kask, P. (1993) *Eur. Biophys. J.*, **22**, 169-175.
40. Rigler, R., Pramanik, A., Jonasson, P., Kratz, G., Jansson, O. T., Nygren, P., Stahl, S., Ekberg, K., Johansson, B., Uhlen, S., Uhlen, M., Jornvall, H., and Wahren, J. (1999) *Proc. Natl. Acad. Sci. USA*, **96**, 13318-13323.
41. Denk, W., Strickler, J. H., and Webb, W. W. (1990) *Science*, **248**, 73-76.
42. Schwille, P., Haupts, U., Maiti, S., and Webb, W. W. (1999) *Biophys. J.*, **77**, 2251-2265.
43. Koppel, D. E. (1974) *Phys. Rev. A*, **10**, 1938-1945.
44. Kask, P., Gunther, R., and Axhausen, P. (1997) *Eur. Biophys. J.*, **25**, 163-169.
45. Qian, H. (1990) *Biophys. Chem.*, **38**, 49-57.
46. Meseth, U., Wohland, T., Rigler, R., and Vogel, H. (1999) *Biophys. J.*, **76**, 1619-1631.
47. Kask, P., Palo, K., Ullmann, D., and Gall, K. (1999) *Proc. Natl. Acad. Sci. USA*, **96**, 13756-13761.
48. Chen, Y., Muller, J. D., So, P. T., and Gratton, E. (1999) *Biophys. J.*, **77**, 553-567.
49. Chen, Y., Muller, J. D., Tetin, S. Y., Tyner, J. D., and Gratton, E. (2000) *Biophys. J.*, **79**, 1074-1084.
50. Enderlein, J., Gregor, I., Patra, D., Dertinger, T., and Kaupp, U. B. (2005) *Chemphyschem.*, **6**, 2324-2336.
51. Ruettinger, S., Buschmann, V., Kramer, B., Erdmann, R., Macdonald, R., and Koberling, F. (2007) *Proc. SPIE*, **6630**, 66300D.
52. Sachl, R., Mikhalyov, I., Hof, M., and Johansson, L. B. (2009) *Phys. Chem. Chem. Phys.*, **11**, 4335-4343.
53. Petrasek, Z., and Schwille, P. (2008) *Biophys. J.*, **94**, 1437-1448.
54. Gendron, P. O., Avaltroni, F., and Wilkinson, K. J. (2008) *J. Fluoresc.*, **18**, 1093-1101.
55. Gosch, M., Blom, H., Holm, J., Heino, T., and Rigler, R. (2000) *Anal. Chem.*, **72**, 3260-3265.
56. Muller, J. D., Chen, Y., and Gratton, E. (2000) *Biophys. J.*, **78**, 474-486.
57. Qian, H., and Elson, E. L. (1990) *Biophys. J.*, **57**, 375-380.
58. Eid, J. S., Mueller, J. D., and Gratton, E. (2000) *Rev. Sci. Instrum.*, **71**, 361-368.
59. Chen, Y., Muller, J. D., Ruan, Q., and Gratton, E. (2002) *Biophys. J.*, **82**, 133-144.
60. Chen, Y., Wei, L. N., and Muller, J. D. (2003) *Proc. Natl. Acad. Sci. USA*, **100**, 15492-15497.
61. Egea, P. F., Rochel, N., Birck, C., Vachette, P., Timmins, P. A., and Moras, D. (2001) *J. Mol. Biol.*, **307**, 557-576.
62. Yu, L., Tan, M., Ho, B., Ding, J. L., and Wohland, T. (2006) *Anal. Chim. Acta*, **556**, 216-225.
63. Tjernberg, L. O., Pramanik, A., Bjorling, S., Thyberg, P., Thyberg, J., Nordstedt, C., Berndt, K. D., Terenius, L., and Rigler, R. (1999) *Chem. Biol.*, **6**, 53-62.
64. Sengupta, P., Garai, K., Sahoo, B., Shi, Y., Callaway, D. J., and Maiti, S. (2003) *Biochemistry*, **42**, 10506-10513.
65. Garai, K., Sureka, R., and Maiti, S. (2007) *Biophys. J.*, **92**, L55-L57.
66. Gerard, M., Debyser, Z., Desender, L., Kahle, P. J., Baert, J., Baekelandt, V., and Engelborghs, Y. (2006) *FASEB J.*, **20**, 524-526.
67. Conway, K. A., Harper, J. D., and Lansbury, P. T. (1998) *Nat. Med.*, **4**, 1318-1320.
68. Sevenich, F. W., Langowski, J., Weiss, V., and Rippe, K. (1998) *Nucleic Acids Res.*, **26**, 1373-1381.
69. Lagerkvist, A. C., Foldes-Papp, Z., Persson, M. A., and Rigler, R. (2001) *Protein Sci.*, **10**, 1522-1528.
70. Tetin, S. Y., Swift, K. M., and Matayoshi, E. D. (2002) *Anal. Biochem.*, **307**, 84-91.
71. Varriale, A., Staiano, M., Iozzino, L., Severino, L., Anastasio, A., Cortesi, M. L., and D'Auria, S. (2009) *Protein Pept. Lett.*, **16**, 1425-1428.
72. Kinjo, M., and Rigler, R. (1995) *Nucleic Acids Res.*, **23**, 1795-1799.

73. Schwille, P., Oehlenschlager, F., and Walter, N. G. (1996) *Biochemistry*, **35**, 10182-10193.
74. Rusu, L., Gambhir, A., McLaughlin, S., and Radler, J. (2004) *Biophys. J.*, **87**, 1044-1053.
75. Yu, L., Ding, J. L., Ho, B., and Wohland, T. (2005) *Biochim. Biophys. Acta*, **1716**, 29-39.
76. Posokhov, Y. O., Rodnin, M. V., Lu, L., and Ladokhin, A. S. (2008) *Biochemistry*, **47**, 5078-5087.
77. Antonenko, Y. N., Perevoshchikova, I. V., Davydova, L. I., Agapov, I. A., and Bogush, V. G. (2010) *Biochim. Biophys. Acta*, **1798**, 1172-1178.
78. Clamme, J. P., Azoulay, J., and Mely, Y. (2003) *Biophys. J.*, **84**, 1960-1968.
79. Pramanik, A., Thyberg, P., and Rigler, R. (2000) *Chem. Phys. Lipids*, **104**, 35-47.
80. Takakuwa, Y., Pack, C. G., An, X. L., Manno, S., Ito, E., and Kinjo, M. (1999) *Biophys. Chem.*, **82**, 149-155.
81. Rhoades, E., Ramlall, T. F., Webb, W. W., and Eliezer, D. (2006) *Biophys. J.*, **90**, 4692-4700.
82. Krasnovsky, A. A. (2004) *Biofizika*, **49**, 305-321.
83. Valenzeno, D. P. (1987) *Photochem. Photobiol.*, **46**, 147-160.
84. Pashkovskaya, A. A., Maizlish, V. E., Shaposhnikov, G. P., Kotova, E. A., and Antonenko, Y. N. (2008) *Biochim. Biophys. Acta*, **1778**, 541-548.
85. Pashkovskaya, A. A., Perevoshchikova, I. V., Maizlish, V. E., Shaposhnikov, G. P., Kotova, E. A., and Antonenko, Yu. N. (2009) *Biochemistry (Moscow)*, **74**, 1021-1026.
86. Allen, N. W., and Thompson, N. L. (2006) *Cytometry A*, **69**, 524-532.
87. Van den Bogaart, G., Hermans, N., Krasnikov, V., de Vries, A. H., and Poolman, B. (2007) *Biophys. J.*, **92**, 1598-1605.
88. Ramadurai, S., Holt, A., Krasnikov, V., van den Bogaart, G., Killian, J. A., and Poolman, B. (2009) *J. Am. Chem. Soc.*, **131**, 12650-12656.
89. Schwille, P., Korlach, J., and Webb, W. W. (1999) *Cytometry*, **36**, 176-182.
90. Korlach, J., Schwille, P., Webb, W. W., and Feigenson, G. W. (1999) *Proc. Natl. Acad. Sci. USA*, **96**, 8461-8466.
91. Wawrezinieck, L., Rigneault, H., Marguet, D., and Lenne, P. F. (2005) *Biophys. J.*, **89**, 4029-4042.
92. Humpolickova, J., Gielen, E., Benda, A., Fagulova, V., Vercammen, J., Vandeven, M., Hof, M., Ameloot, M., and Engelborghs, Y. (2006) *Biophys. J.*, **91**, L23-L25.
93. Wenger, J., Conchonaud, F., Dintinger, J., Wawrezinieck, L., Ebbesen, T. W., Rigneault, H., Marguet, D., and Lenne, P. F. (2007) *Biophys. J.*, **92**, 913-919.
94. Chiantia, S., Ries, J., and Schwille, P. (2009) *Biochim. Biophys. Acta*, **1788**, 225-233.
95. Przybylo, M., Sykora, J., Humpolickova, J., Benda, A., Zan, A., and Hof, M. (2006) *Langmuir*, **22**, 9096-9099.
96. Machan, R., and Hof, M. (2010) *Int. J. Mol. Sci.*, **11**, 427-457.
97. Politz, J. C., Browne, E. S., Wolf, D. E., and Pederson, T. (1998) *Proc. Natl. Acad. Sci. USA*, **95**, 6043-6048.
98. Ries, J., Yu, S. R., Burkhardt, M., Brand, M., and Schwille, P. (2009) *Nat. Methods*, **6**, 643-645.
99. Oehlenschlager, F., Schwille, P., and Eigen, M. (1996) *Proc. Natl. Acad. Sci. USA*, **93**, 12811-12816.
100. Walter, N. G., Schwille, P., and Eigen, M. (1996) *Proc. Natl. Acad. Sci. USA*, **93**, 12805-12810.
101. Schwille, P., Meyer-Almes, F. J., and Rigler, R. (1997) *Biophys. J.*, **72**, 1878-1886.
102. Haupts, U., Maiti, S., Schwille, P., and Webb, W. W. (1998) *Proc. Natl. Acad. Sci. USA*, **95**, 13573-13578.
103. Persson, G., Thyberg, P., and Widengren, J. (2008) *Biophys. J.*, **94**, 977-985.
104. Sanden, T., Salomonsson, L., Brzezinski, P., and Widengren, J. (2010) *Proc. Natl. Acad. Sci. USA*, **107**, 4129-4134.
105. Magzoub, M., Padmawar, P., Dix, J. A., and Verkman, A. S. (2006) *J. Phys. Chem. B*, **110**, 21216-21221.
106. Al Soufi, W., Reija, B., Novo, M., Felekyan, S., Kuhnemuth, R., and Seidel, C. A. (2005) *J. Am. Chem. Soc.*, **127**, 8775-8784.
107. Bonnet, G., Krichevsky, O., and Libchaber, A. (1998) *Proc. Natl. Acad. Sci. USA*, **95**, 8602-8606.
108. Kim, H. D., Nienhaus, G. U., Ha, T., Orr, J. W., Williamson, J. R., and Chu, S. (2002) *Proc. Natl. Acad. Sci. USA*, **99**, 4284-4289.
109. Shusterman, R., Gavrinyov, T., and Krichevsky, O. (2008) *Phys. Rev. Lett.*, **100**, 98-102.
110. Chattopadhyay, K., Saffarian, S., Elson, E. L., and Frieden, C. (2002) *Proc. Natl. Acad. Sci. USA*, **99**, 14171-14176.
111. Neuweiler, H., Johnson, C. M., and Fersht, A. R. (2009) *Proc. Natl. Acad. Sci. USA*, **106**, 18569-18574.
112. Dittrich, P. S., and Schwille, P. (2002) *Anal. Chem.*, **74**, 4472-4479.
113. Kuricheti, K. K., Buschmann, V., and Weston, K. D. (2004) *Appl. Spectrosc.*, **58**, 1180-1186.
114. Brister, P. C., Kuricheti, K. K., Buschmann, V., and Weston, K. D. (2005) *Lab. Chip.*, **5**, 785-791.
115. Edel, J. B., and de Mello, A. J. (2003) *Anal. Sci.*, **19**, 1065-1069.
116. Okagbare, P. I., and Soper, S. A. (2009) *Analyst*, **134**, 97-106.
117. Park, H. Y., Qiu, X., Rhoades, E., Korlach, J., Kwok, L. W., Zipfel, W. R., Webb, W. W., and Pollack, L. (2006) *Anal. Chem.*, **78**, 4465-4473.
118. Van Orden, A., and Keller, R. A. (1998) *Anal. Chem.*, **70**, 4463-4471.
119. LeCaptain, D. J., and van Orden, A. (2002) *Anal. Chem.*, **74**, 1171-1176.
120. Bayer, J., and Radler, J. O. (2006) *Electrophoresis*, **27**, 3952-3963.
121. Fogarty, K., and van Orden, A. (2009) *Methods*, **47**, 151-158.
122. Pan, X., Yu, H., Shi, X., Korzh, V., and Wohland, T. (2007) *J. Biomed. Opt.*, **12**, 14-34.
123. Malone, M. H., Sciaky, N., Stalheim, L., Hahn, K. M., Linney, E., and Johnson, G. L. (2007) *BMC Biotechnol.*, **7**, 40.
124. Van Craenenbroeck, E., Matthys, G., Beirlant, J., and Engelborghs, Y. (1999) *J. Fluoresc.*, **9**, 325-331.
125. Van Craenenbroeck, E., and Engelborghs, Y. (2000) *J. Mol. Recognit.*, **13**, 93-100.
126. Van Rompaey, E., Sanders, N., de Smedt, S. C., Demeester, J., van Craenenbroeck, E., and Engelborghs, Y. (2000) *Macromolecules*, **33**, 8280-8288.
127. Van Rompaey, E., Engelborghs, Y., Sanders, N., de Smedt, S. C., and Demeester, J. (2001) *Pharm. Res.*, **18**, 928-936.

128. Van den Bogaart, G., Mika, J. T., Krasnikov, V., and Poolman, B. (2007) *Biophys. J.*, **93**, 154-163.
129. Van den Bogaart, G., Kusters, I., Velasquez, J., Mika, J. T., Krasnikov, V., Driessen, A. J., and Poolman, B. (2008) *Methods*, **46**, 123-130.
130. Van den Bogaart, G., Guzman, J. V., Mika, J. T., and Poolman, B. (2008) *J. Biol. Chem.*, **283**, 33854-33857.
131. Pashkovskaya, A., Kotova, E., Zorlu, Y., Dumoulin, F., Ahsen, V., Agapov, I., and Antonenko, Y. (2010) *Langmuir*, **26**, 5726-5733.
132. Smith, P. B., Dendramis, K. A., and Chiu, D. T. (2010) *Langmuir*, **26**, 10218-10222.
133. Van den Bogaart, G., Krasnikov, V., and Poolman, B. (2007) *Biophys. J.*, **92**, 1233-1240.
134. Kusters, I., van den Bogaart, G., de Wit, J., Krasnikov, V., Poolman, B., and Driessen, A. (2010) *Methods Mol. Biol.*, **619**, 131-143.
135. Perevoshchikova, I. V., Zorov, D. B., and Antonenko, Y. N. (2008) *Biochim. Biophys. Acta*, **1778**, 2182-2190.
136. Perevoshchikova, I. V., Zorov, S. D., Kotova, E. A., Zorov, D. B., and Antonenko, Y. N. (2010) *FEBS Lett.*, **584**, 2397-2402.
137. Meyer, T., and Schindler, H. (1988) *Biophys. J.*, **54**, 983-993.
138. Berland, K. M., So, P. T., Chen, Y., Mantulin, W. W., and Gratton, E. (1996) *Biophys. J.*, **71**, 410-420.
139. Levi, V., Ruan, Q., Kis-Petikova, K., and Gratton, E. (2003) *Biochem. Soc. Trans.*, **31**, 997-1000.
140. Lu, H. P. (2005) *Acc. Chem. Res.*, **38**, 557-565.
141. Novoderezhkin, V. I., Rutkauskas, D., and van Grondelle, R. (2006) *Biophys. J.*, **90**, 2890-2902.
142. Osad'ko, I. S. (2006) *Phys.-Usp.*, **49**, 19-51.
143. Mukhopadhyay, S., and Deniz, A. A. (2007) *J. Fluoresc.*, **17**, 775-783.
144. Hilario, J., and Kowalczykowski, S. C. (2010) *Curr. Opin. Chem. Biol.*, **14**, 15-22.